Probing charged lepton flavor violation and quantum entanglement in muon on-target experiments

Leyun Gao[1,2] for the PKMuon Collaboration[*]

[1]State Key Laboratory of Nuclear Physics and Technology, Peking University

[2]School of Physics, Peking University

MIP 2025, Changsha, China May 18, 2025

Based primarily on: arXiv:2410.20323, arXiv:2411.12518, arXiv:2502.07597, and arXiv:2503.22956

[*]https://lyazj.github.io/pkmuon-site/categories/activities/ and [1–5]

Outline

Outline

The PKMuon Experiment

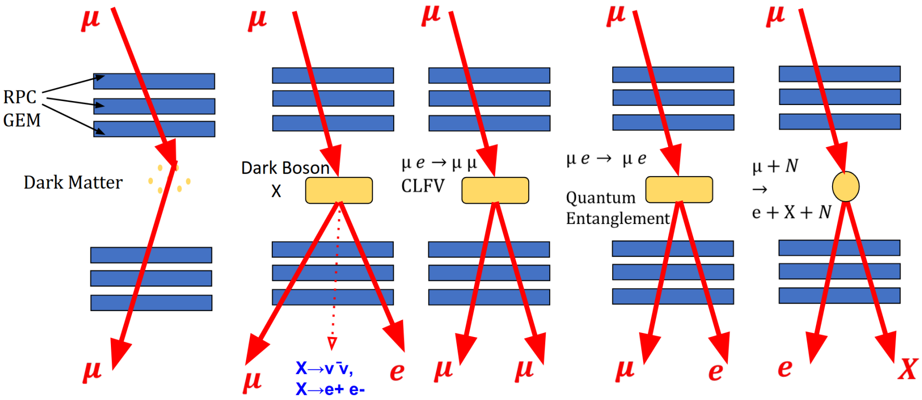

Read more in Qiang Li's talk yesterday.

PKMuon detector simulation framework

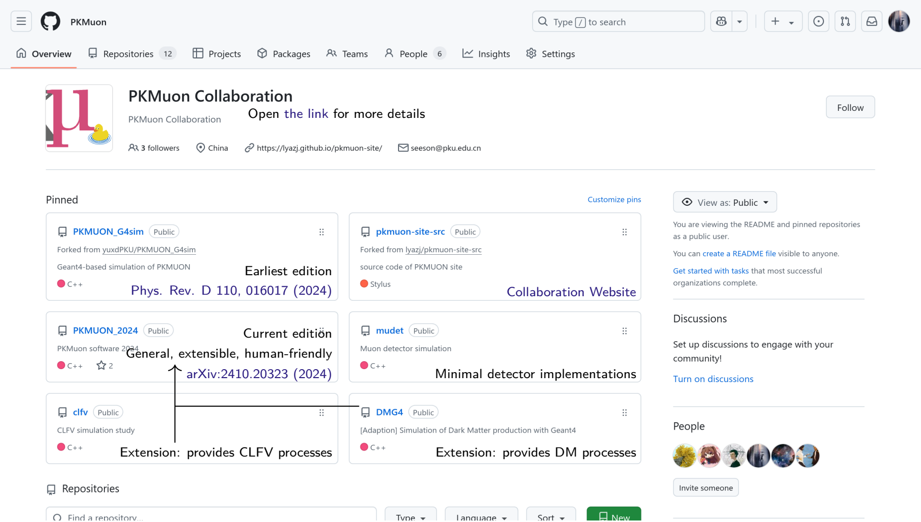

Outline

CLFV and recent studies

CLFV (Charged Lepton Flavor Violation):

- Strongly suppressed due to the tiny neutrino masses in the Standard Model (SM): $\mathrm{BR}(\mu \to e\gamma) \sim 10^{-54}$–$10^{-55}$
- Can be significantly enhanced in various BSM models

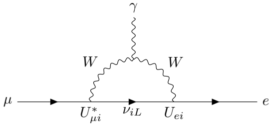

FIG. SM $\mu \to e\gamma$ decay process

Dedicated low-energy muon experiments, such as $\mu \to e\gamma$, set limits on $\lambda_{ee}\lambda_{e\mu}$ and $\lambda_{e\mu}\lambda_{\mu\mu}$ coherently according to Ref. [6] as

$$\Gamma(\mu \to e\gamma) = \frac{\alpha G_F^2 m_\mu^3 M_Z^4 \left(\sin^2\theta_W \left(\sin^2\theta_W - 1/2\right)\right)^2}{4\pi^4 M_{Z'}^4} \left(\lambda_{ee}\lambda_{e\mu}m_e + \lambda_{e\mu}\lambda_{\mu\mu}m_\mu + \lambda_{e\tau}\lambda_{\tau\mu}m_\tau + \ldots\right)^2,$$

The gray part involving τ and BSM contributions is not considered in previous works.

Strong interference and cancellation between the terms shown or omitted are possible, allowing the existence of terms with very large modulus, highlighting the necessity to probe each term individually.

Theoretical model and simulation setup

The $U(1)$ Z' CLFV model:

- Has the same gauge coupling and chiral strength as the SM Z boson except for allowing CLFV quantified by

$$\lambda = \begin{pmatrix} \lambda_{ee} & \lambda_{e\mu} & \lambda_{e\tau} \\ \lambda_{\mu e} & \lambda_{\mu\mu} & \lambda_{\mu\tau} \\ \lambda_{\tau e} & \lambda_{\tau\mu} & \lambda_{\tau\tau} \end{pmatrix},$$

relative to SM, with the diagonal elements equal to 1 and the off-diagonal expected to be near 0

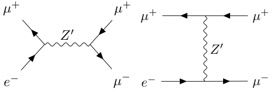

FIG. $U(1)$ Z'-mediated CLFV processes

The PKMuon detectors for $\mu^+ e^- \to \mu^+ \mu^-$ measurements:

- Applies to cosmic-ray and artificial muons
- Cost-effective: no magnetic/calorimeter, giving 2 average momentum directions for each track, without magnitudes
- 3 RPCs per group to suppress muon decay products
- A scintillator PID system downstream RPCs to reject (ionization/bremsstrahlung) electrons (not plotted)
- Generalizable (from DM detection) to other experiments

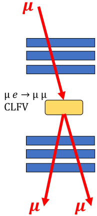

FIG. PKMuon RPC tracker for CLFV measurements

Efficient new physics modeling

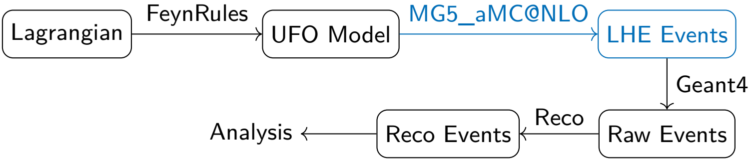

LHE events for arbitrary new physics can be efficiently and conveniently generated through FeynRules and MG5_aMC@NLO

- For various Z' masses and incoming muon energies (incoming muon energies should be varied for muons passing the first 3 RPC layers)
- However, efficient only for *bunch of* (at least $\sim 10^4$) events per mass/energy setup

Our speeding-up solution to avoid event-by-event launch of MG5_aMC@NLO

Pre-acquire the cross section and kinematic distributions for interpolation.

Efficient new physics modeling

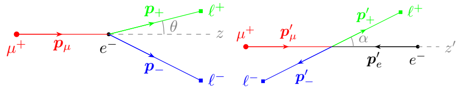

FIG. Lab and COM frame event display

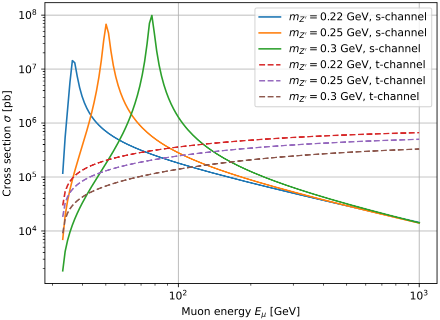

FIG. s- and t-channel cross sections

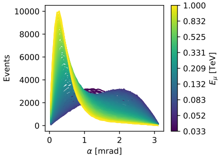

(a) $m_{Z'} = 0.22$ GeV

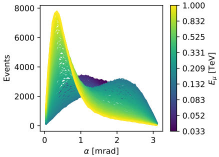

(b) $m_{Z'} = 0.30$ GeV

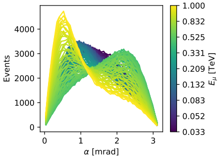

(c) $m_{Z'} = 0.50$ GeV

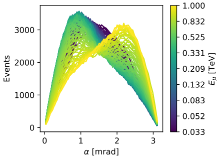

(d) $m_{Z'} = 0.80$ GeV

FIG. $\mu^+ e^- \to \mu^+ \mu^-$ event distributions in the COM frame with varying incident E_μ.

Efficient new physics modeling

Algorithm: Efficient $\mu^+e^- \to \ell^+\ell^-$ event generation

function $\textsc{GenerateMuELL}(E_\mu, \vec{p}_\mu, m_\ell)$
  $E_{\mu 1}, E_{\mu 2}, \sigma_1, \sigma_2, H_1, H_2 \leftarrow$ $\textsc{AdjacentGridPoints}(E_\mu)$;
  if E_μ is out of the grid range **then**
    return no $\mu^+e^- \to \ell^+\ell^-$ happens;
  end if
  $w_1 \leftarrow \frac{E_\mu - E_{\mu 2}}{E_{\mu 1} - E_{\mu 2}}$, $w_2 \leftarrow \frac{E_{\mu 1} - E_\mu}{E_{\mu 1} - E_{\mu 2}}$;
  $\sigma \leftarrow w_1\sigma_1 + w_2\sigma_2$; // cross section
  if $\textsc{Random}(0,1) < w_1$ **then**
    $\alpha \leftarrow H_1.\textsc{Sample}()$; // polar angle
  else
    $\alpha \leftarrow H_2.\textsc{Sample}()$;
  end if
  $\phi \leftarrow \textsc{Random}(0, 2\pi)$; // azimuthal angle
  $E', p', \gamma, \beta \leftarrow \textsc{Kinematics}(E_\mu, m_\ell)$;
  $p_{x+} \leftarrow p' \sin\alpha \cos\phi$, $p_{y+} \leftarrow p' \sin\alpha \sin\phi$;
  $p_{z+} \leftarrow \gamma\,(p' \cos\alpha + \beta E'/2)$;
  $\vec{p}_+ \leftarrow \textsc{ThreeVector}(p_{x+}, p_{y+}, p_{z+})$;
  $\vec{p}_+ \leftarrow \vec{p}_+.\textsc{RotateZAxisTo}(\hat{p}_\mu)$;
  $\vec{p}_- \leftarrow \vec{p}_\mu - \vec{p}_+$;
  return $\sigma, \vec{p}_+, \vec{p}_-$;
end function

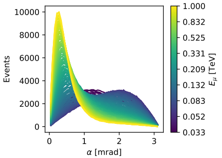

(a) $m_{Z'} = 0.22$ GeV

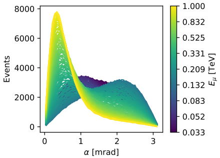

(b) $m_{Z'} = 0.30$ GeV

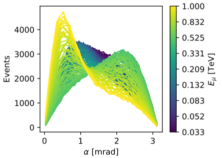

(c) $m_{Z'} = 0.50$ GeV

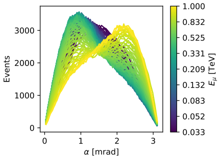

(d) $m_{Z'} = 0.80$ GeV

FIG. $\mu^+e^- \to \mu^+\mu^-$ event distributions in the COM frame with varying incident E_μ.

Detector simulation with background

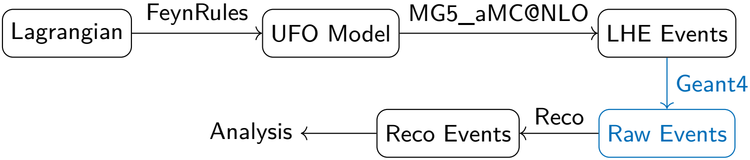

Background-included signal detection simulated by Geant4 11.2.2:

- $\mu^+ e^- \to \ell^+ \ell^-$: subclasses `G4VDiscreteProcess`
- Simulated upon physics list `FTFP_BERT`
- Signal (or background) definition: whether (or not) CLFV happens
- Signal rate is scaled to 10^{-3} to 10^{-2} to balance precision and efficiency
- Allows a step length up to 10^{-3} times MFP assuring granularity

Detector simulation with background

The PKMuon RPC tracking detectors:

- 3 RPCs/group $\times$ 2 groups
- minor/major distance as 200/500 mm
- 2D pixel readout (0.7 mm Exp., 0.5 mm MC)
- trigger as 1 MeV (1/2 mean muon Edep.)

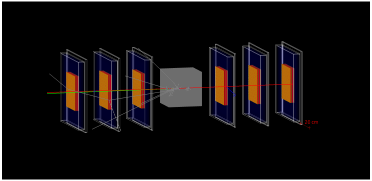

FIG. $\mu^+ e^- \to \mu^+ \mu^-$ event display

CLFV *can* happen outside the target, but those events are unintended for measurements and will be filtered out by event selection.

The parameters here and the target selection are to be optimized.

Since the measurement is insensitive to the focusing of the incoming muon beam, the beam is considered to be monochromatic, impinging perpendicularly to the detector and distributed uniformly over the area of the RPC module.

Event reconstruction and selection

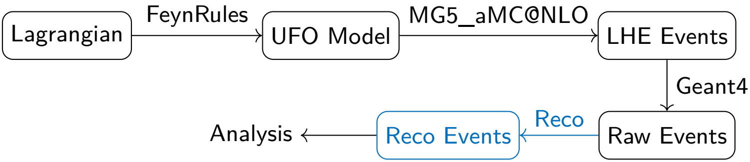

Pre-requirements:

- Comparing none/perfect electron rejection
- #hits on RPCs 0–5: [1, 1, 1, 2, 2, 2]

Reconstruction of 2 outgoing tracks:

- Step 1/3: match hits on RPC 3 and 5
  - expecting 2 tracks diverge from a single point
  - i.e. minimizing the sum of the 2 resulting track lengths
  - e.g. $BF + AE < BE + AF$
- Step 2/3: add hits on RPC 4, minimizing total χ^2 error
- Step 3/3: Recompute (fit) spatial lines BDF and ACE

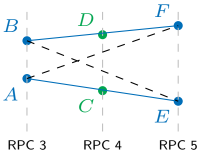

Event reconstruction and selection

Event distribution:

- key signal feature: 3 highly collimated tracks (in: 0; out: 1, 2)
- distributed discretely due to limited detector granularity
- signal and background remain largely separated

Event selection:

- $\chi^2 \leq 6$
- $\max_{i \neq j} \langle \vec{p}_i, \vec{p}_j \rangle \leq 0.003$

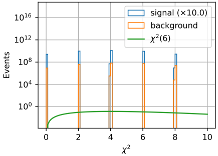

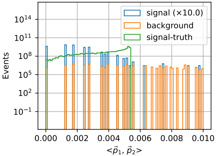

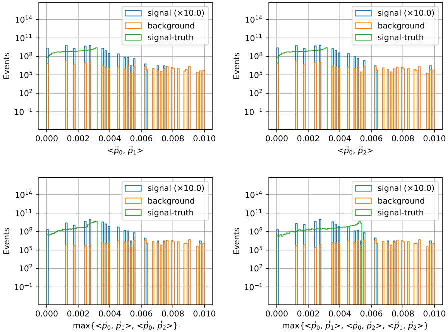

FIG. Event distributions for $E_\mu = 50.2$ GeV, $m_{Z'} = 0.25$ GeV, and $\lambda_{e\mu}$ scaled to 10. The target is a 30 mm thick aluminum block. The yields are normalized to 3×10^{13} muons on target, corresponding to a one-year run.

Results and discussion

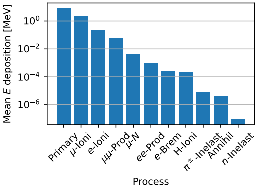

FIG. Typical background components (almost all e!)

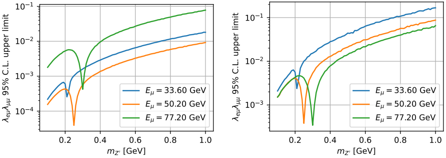

FIG. Prospected 95% ULs for 3 cm Al (L) and 8 cm Pb (R) targets, with e-veto, for a one-year run

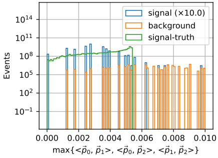

(a) 3 cm Al

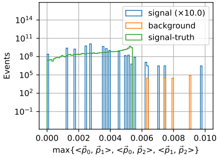

(b) 3 cm Al, with e-veto

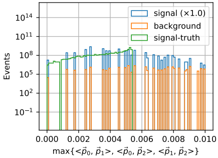

(c) 8 cm Pb

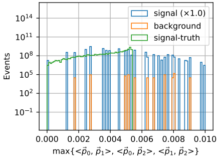

(d) 8 cm Pb, with e-veto

FIG. Event distribution before final selection

Background events are vanishing, raising requirements on a higher statistics in the future. Finer selection can also be enabled in a higher statistics.

Outline

The current absence of free-traveling leptons in QE measurements

- The ATLAS and CMS Collaborations recently observed quantum entanglement involving **top quarks** at a center-of-mass energy of 13 TeV, marking the highest energy measurements of quantum entanglement to date [15–18]
- Most studies on charged lepton QE have concentrated on the decaying **tau** leptons [19–25], while less attention has been given to electrons and muons
- Solid-state quantum computation was established in 2005 with **electron pairs confined in semiconductor quantum dots** [26]: entangled states were prepared, coherently manipulated, and measured
- **No similar experiment has been done with free-traveling electrons** as measuring the spin of a single traveling electron poses a significant challenge due to interference from its orbital motion [27]

Our proposal

Conduct a **first** measurement of the polarization correlation between charged lepton beams through joint measurements of their individual polarization-sensitive scatterings off two separate targets.

Outline

Theory: Concurrence, CHSH inequality, and the kinematic approach

- Entanglement can be quantified by *concurrence* [28–30], defined as

$$\mathcal{C}(\rho_f) = \max\{0, \lambda_1 - \lambda_2 - \lambda_3 - \lambda_4\} \in [0, 1] \quad (1)$$

  for a two-qubit system, where λ_i $(\lambda_i \geq \lambda_j,\ \forall i < j)$ are the square roots of the eigenvalues of the matrix $\rho_f(\sigma_2 \otimes \sigma_2)\rho_f^*(\sigma_2 \otimes \sigma_2)$. If $\mathcal{C} > 0$, the two-qubit system is entangled.

- The *CHSH inequality*, $I_2 \leq 2$ [31], is the Bell inequality for a two-qubit system. The optimal (maximal) I_2 [32] evaluates to

$$I_2 = 2\sqrt{\lambda_1 + \lambda_2}, \quad (2)$$

  where λ_1 and λ_2 are the two largest eigenvalues of the matrix $C^{\mathrm{T}}C$, and C is the correlation matrix calculated by $C_{ij} = \mathrm{Tr}\left(\rho_f\left(\sigma_i \otimes \sigma_j\right)\right)$. $I_2 = 2\sqrt{2}$ is the upper limit of the quantum mechanics.

- In addition to the *decay approach* used for decaying particles, the *kinematic approach* [33, 34] can reconstruct quantum states from production kinematics, applicable to stable particles produced in simple QED scatterings.

Electron-muon entanglement sources via muon on-target experiments

Concurrence $\mathcal{C}(\rho_f)$:

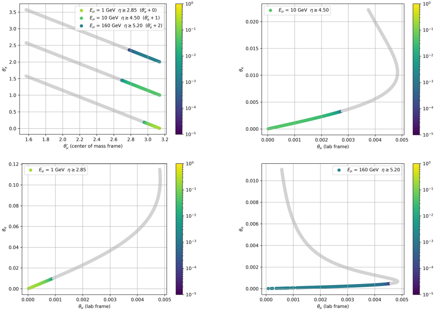

Optimal I_2:

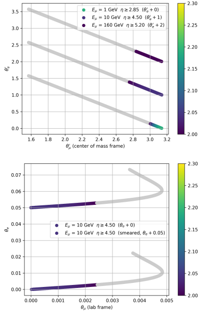

- Simulated by MG5_aMC@NLO 3.5.5 [35] in tree-level QED with non-zero lepton masses
- The light gray regions depict $\mathcal{C}(\rho_f) = 0$ or $I_2 \leq 2$
- Assuming a **1-day** run with a **10 GeV** muon beam of flux $\mathbf{10^5}$**/s** on 10 cm Al targets, the expected number of events with $\mathcal{C}(\rho_f) > 0$ is $\mathbf{2.6 \times 10^4}$

$E_{\rm beam}$/GeV	$E_{\rm COM}$/GeV	$\mathcal{C}(\rho_f)_{\max}$	$\theta_{\mu,\max}$/mrad	$\theta_{e,\max}$/mrad	$E_{\mu,\min}$/GeV	$E_{e,\min}$/GeV	$\sigma_{\rm E}$/μb	$\sigma_{{\rm E},\,\theta\geq 0.5\,{\rm mrad}}$/μb
1	0.111	**0.22**	0.9	10.2	0.92	0.08	0.56	0.56
10	0.146	**0.044**	**2.8**	**3.3**	**5.2**	**4.5**	**0.39**	**0.39**
160	0.418	0.0014	4.6	0.5	10	145	0.027	0.022

Electron-positron entanglement sources via positron on-target experiments

Concurrence $\mathcal{C}(\rho_f)$:

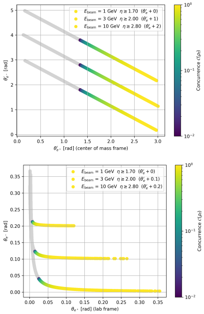

Optimal I_2:

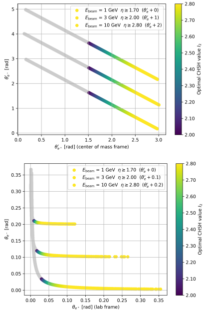

- The angular ranges exhibiting $\mathcal{C}(\rho_f) > 0$ in the center-of-mass frame are significantly broader
- The theoretical upper limits for both $\mathcal{C}(\rho_f)$ and I_2 in quantum mechanics are nearly reached as θ'_{e^+} approaches 3
- Assuming a **1 GeV** positron beam with a flux of $\mathbf{10^{12}}$**/s** directed at a 10 cm thick Al target, the expected entangled event rate is $\mathbf{1.9 \times 10^9/s}$
- A golden region for measurements:
  - $E_{\text{beam}} = \mathbf{1\ GeV}$, 0.05 rad $\leq \theta_{e^+} \leq 0.1$ rad
  - 23.4% of all events with $\mathcal{C}(\rho_f) > 0$
  - $E \geq \mathbf{0.094\ GeV}$, $\theta \geq \mathbf{0.0103\ rad}$
  - $\mathcal{C}(\rho_f)$ reaching up to $\mathbf{0.953}$ and I_2 up to $\mathbf{2.8281}$

E_{beam}/GeV	E_{COM}/GeV	$\mathcal{C}^{\max}(\rho_f)$	$I_2^{\max}$	$E_{e^+}^{\min}$/GeV	$E_{e^-}^{\min}$/GeV	$\theta_{e^+}^{\min}$/rad	$\theta_{e^-}^{\min}$/rad	σ_{E}/μb
1	0.032	0.9996	2.8281	0.008	0.389	0.0255	0.0028	243.6
3	0.055	0.9997	2.8282	0.023	1.166	0.0147	0.0016	82.1
10	0.101	0.9997	2.8282	0.074	3.890	0.0081	0.0009	26.5

A first electron-positron beam correlation measurement proposal

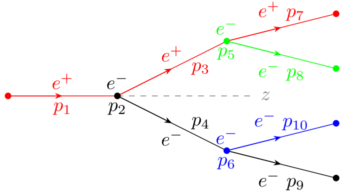

FIG. Proposed cascade experiment for measuring polarization correlations of the primary products

Simulation setup:

- $0.05 \text{ rad} \leq \theta_3 \leq 0.1 \text{ rad}$ in a 1 GeV positron on-target experiment
- The spins of target electrons 5 and 6 are aligned with the beam direction
- Consider the main component of the primary state, $(LL + RR)/\sqrt{2}$

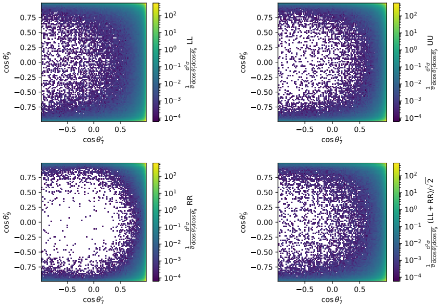

FIG. Joint angular distribution densities of the two secondary scattering processes

Assuming the two secondary targets are 10 cm thick iron, the event rate in $\cos\theta'_7 \leq 0.5 \wedge -0.75 \leq \theta'_9 \leq 0.75$ is $\mathbf{1.4 \times 10^2}$/s for the state $(LL + RR)/\sqrt{2}$.

Future prospects: Scattering-based simplified state tomography

Take $0.05\ \mathrm{rad} \leq \theta_3 \leq 0.1\ \mathrm{rad}$ in a 1 GeV positron on-target experiment as an example:

- The state of the primary products is approximately 1% $(RL+LR)/\sqrt{2}$, 1% $(RL-LR)/\sqrt{2}$, 7% $(RR-LL)/\sqrt{2}$, and 90% $(RR+LL)/\sqrt{2}$ in the lab frame
- The optimized ratio of the yields of $(LL+RR)/\sqrt{2}$ to UU is $1.29 \pm 0.03(\mathrm{MC})$, corresponding to 4.4×10^3 post-optimization efficient signal event counts and an expected signal yield over a **27-second** run; the result for $(LR+RL)/\sqrt{2}$ is $0.78 \pm 0.02(\mathrm{MC})$ in comparison
- Other uncertainties, such as those from process modeling and background suppression, may dominate the real experimental analysis
- For the 20% polarized targets, the ratios are 1.010 ± 0.009 and 0.986 ± 0.009 generated from 25 times the number of Monte Carlo events, corresponding to 2.5×10^4 efficient event counts accumulated in **680 seconds**
- The high event rate can help mitigate the decline in resolving power associated with low target polarization purities in real-world applications
- **A simplified state tomography can be performed assuming prior knowledge from the primary scattering**

Outline

Summary

PKMuon CLFV experiment:

- Exclusively sensitive to $\lambda_{e\mu}\lambda_{\mu\mu}$
- A novel and generalizable efficient event generation algorithm
- $\mu^+e^- \to \mu^+\mu^-$ simulation shows the expected 95% CL UL on $\lambda_{e\mu}\lambda_{\mu\mu} \sim 10^{-5}$ with Z' mass ~ 0.25 GeV for a one-year run
- Comparable with the LHE-level simulation in Ref. [7] (figure on the right)

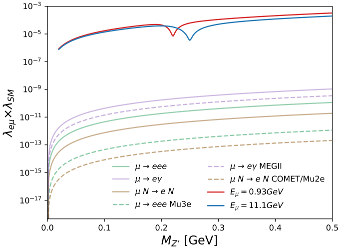

PKMuon quantum entanglement experiment:

- GeV-scale muon and positron on-target experiments as **controllable entangled lepton pair sources**
- Quantum entanglement and the CHSH inequality violation are present
- A **first measurement of the correlation between entangled free-traveling lepton pairs** is proposed to verify the entanglement

Thanks for your attention!

References I

[1] Xudong Yu et al. Proposed Peking University muon experiment for muon tomography and dark matter search. *Phys. Rev. D*, 110(1):016017, 2024.

[2] Leyun Gao, Zijian Wang, Cheng-en Liu, Jinning Li, Alim Ruzi, Qite Li, Chen Zhou, and Qiang Li. Probing charged lepton flavor violation in an economical muon on-target experiment. 10 2024.

[3] Leyun Gao, Alim Ruzi, Qite Li, Chen Zhou, Liangwen Chen, Xueheng Zhang, Zhiyu Sun, and Qiang Li. Quantum state tomography with muons, 11 2024.

[4] Leyun Gao, Alim Ruzi, Qite Li, Chen Zhou, and Qiang Li. Testing spooky action between free-traveling electron-positron pairs. 2 2025.

[5] Leyun Gao, Cheng-en Liu, Qite Li, Chen Zhou, Qiang Li, Liangwen Chen, Xueheng Zhang, Yu Xu, and Zhiyu Sun. Probing and Knocking with Muons, 3 2025.

[6] Paul Langacker and Michael Plumacher. Flavor changing effects in theories with a heavy Z' boson with family nonuniversal couplings. *Phys. Rev. D*, 62:013006, 2000.

[7] Ran Ding, Jingshu Li, Meng Lu, Zhengyun You, Zijian Wang, and Qiang Li. Study of charged Lepton Flavor Violation in electron muon interactions. *JHEP*, 01:165, 2025.

[8] C. N. Yang. C. S. Wu's Contributions: A Retrospective in 2015. *Int. J. Mod. Phys. A*, 30(20):1530050, 2015.

[9] C. S. Wu and I. Shaknov. The Angular Correlation of Scattered Annihilation Radiation. *Phys. Rev.*, 77:136–136, 1950.

References II

[10] J. S. Bell. On the Einstein-Podolsky-Rosen paradox. *Physics Physique Fizika*, 1:195–200, 1964.

[11] Stuart J. Freedman and John F. Clauser. Experimental Test of Local Hidden-Variable Theories. *Phys. Rev. Lett.*, 28:938–941, 1972.

[12] John F. Clauser and Abner Shimony. Bell's theorem: Experimental tests and implications. *Rept. Prog. Phys.*, 41:1881–1927, 1978.

[13] Popular information: The nobel prize in physics 2022.

[14] MHL Pryce and JC Ward. Angular correlation effects with annihilation radiation. *Nature*, 160(4065):435–435, 1947.

[15] Georges Aad et al. Observation of quantum entanglement with top quarks at the ATLAS detector. *Nature*, 633(8030):542–547, 2024.

[16] Aram Hayrapetyan et al. Observation of quantum entanglement in top quark pair production in proton–proton collisions at $\sqrt{s} = 13$ TeV. *Rept. Prog. Phys.*, 87(11):117801, 2024.

[17] Aram Hayrapetyan et al. Measurements of polarization and spin correlation and observation of entanglement in top quark pairs using lepton+jets events from proton-proton collisions at $\sqrt{s}$ = 13 TeV. 9 2024.

[18] Yoav Afik and Juan Ramón Muñoz de Nova. Entanglement and quantum tomography with top quarks at the LHC. *Eur. Phys. J. Plus*, 136(9):907, 2021.

[19] J. Babson and Ernest Ma. Decay Product Correlation of $\tau^+\tau^-$ From e^+e^- Annihilation. *Phys. Rev. D*, 26:2497, 1982.

References III

[20] Paolo Privitera. Decay correlations in $e^+e^- \to \tau^+\tau^-$ as a test of quantum mechanics. *Phys. Lett. B*, 275:172–180, 1992.

[21] Herbert K. Dreiner. Bell's inequality and tau physics at LEP, 10 1992.

[22] Karl Ehatäht, Marco Fabbrichesi, Luca Marzola, and Christian Veelken. Probing entanglement and testing Bell inequality violation with $\mathrm{e}^+\mathrm{e}^- \to \tau^+\tau^-$ at Belle II. 11 2023.

[23] Kai Ma and Tong Li. Testing Bell inequality through $h \to \tau\tau$ at CEPC. 9 2023.

[24] Mohammad Mahdi Altakach, Priyanka Lamba, Fabio Maltoni, Kentarou Mawatari, and Kazuki Sakurai. Quantum information and CP measurement in $H \to \tau^+\tau^-$ at future lepton colliders. *Phys. Rev. D*, 107(9):093002, 2023.

[25] M. Fabbrichesi and L. Marzola. Quantum tomography with τ leptons at the FCC-ee: Entanglement, Bell inequality violation, sinθW, and anomalous couplings. *Phys. Rev. D*, 110(7):076004, 2024.

[26] J. R. Petta, A. C. Johnson, J. M. Taylor, E. A. Laird, A. Yacoby, M. D. Lukin, C. M. Marcus, M. P. Hanson, and A. C. Gossard. Coherent Manipulation of Coupled Electron Spins in Semiconductor Quantum Dots. *Science*, 309(5744):1116955, 2005.

[27] B. M. Garraway and S. Stenholm. Does a flying electron spin? *Contemporary Physics*, 43(3):147–160, 2002.

[28] William K. Wootters. Entanglement of formation of an arbitrary state of two qubits. *Phys. Rev. Lett.*, 80:2245–2248, 1998.

[29] Robert M. Gingrich and Christoph Adami. Quantum Entanglement of Moving Bodies. *Phys. Rev. Lett.*, 89:270402, 2002.

References IV

[30] Scott Hill and William K. Wootters. Entanglement of a pair of quantum bits. *Phys. Rev. Lett.*, 78:5022–5025, 1997.

[31] John F. Clauser, Michael A. Horne, Abner Shimony, and Richard A. Holt. Proposed experiment to test local hidden variable theories. *Phys. Rev. Lett.*, 23:880–884, 1969.

[32] R. Horodecki, P. Horodecki, and M. Horodecki. Violating Bell inequality by mixed spin-1/2 states: necessary and sufficient condition. *Phys. Lett. A*, 200(5):340–344, 1995.

[33] Samuel Fedida and Alessio Serafini. Tree-level entanglement in quantum electrodynamics. *Phys. Rev. D*, 107(11):116007, 2023.

[34] Kun Cheng, Tao Han, and Matthew Low. Quantum Tomography at Colliders: With or Without Decays. 10 2024.

[35] J. Alwall, R. Frederix, S. Frixione, V. Hirschi, F. Maltoni, O. Mattelaer, H. S. Shao, T. Stelzer, P. Torrielli, and M. Zaro. The automated computation of tree-level and next-to-leading order differential cross sections, and their matching to parton shower simulations. *JHEP*, 07:079, 2014.

PKMuon detector simulation framework

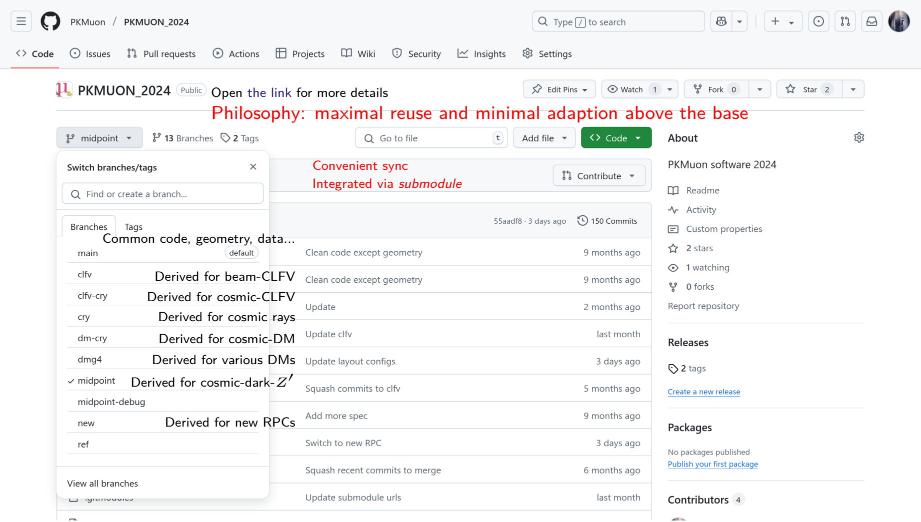

PKMuon detector simulation framework

Files

main

Go to file

- DM_step1
- DM_step2
- analysis
- config
  - layout.yaml
  - layout_al.yaml
  - layout_pb.yaml
  - material_schema.yaml
  - rpc.yaml
  - rpc_material.yaml
  - rpc_readout.yaml
  - volume_schema.yaml
- include
- spec
- src
  - ActionInitialization.cc
  - DetectorConstruction.cc
  - EventAction.cc
  - GeometryConfig.cc
  - GpsPrimaryGeneratorAction.cc

PKMUON_2024 / config / rpc.yaml   Open the link for more details   Top

Code Blame 166 lines (143 loc) · 2.81 KB   Raw

```yaml
      - rpc_glass
    material: rpc_gas

  rpc_electrode_pair:
    solid: bottom_up
    components:
      - rpc_electrode
      - rpc_electric
      - rpc_electrode
    material: rpc_gas

  rpc_electrode_pair_0:
    solid: rotation
    components: [rpc_electrode_pair]

  rpc_electrode_pair_1:
    solid: rotation
    components: [rpc_electrode_pair, [x, 180 deg]]

  rpc_mainbody:
    solid: bottom_up
    components:
      - rpc_x_readout_board  # external
      - rpc_insulating_film
      - rpc_electrode_pair_0
      - rpc_insulating_film
      - rpc_gas
      - rpc_t_readout_board  # external
      - rpc_gas
      - rpc_insulating_film
      - rpc_electrode_pair_1
      - rpc_insulating_film
      - rpc_y_readout_board  # external
    material: rpc_gas
```

GEANT := GEometry ANd Tracking

Abstraction: Multiple geometrical operations supported

Modulization: Accepts external definitions (elsewhere)

Decorrelated from the code; human-friendly; error-repelling

Quantum entanglement measurements — history and today

- As reviewed by C. N. Yang [8], the first experiment on quantum entanglement is the Wu-Shaknov Experiment published in 1950 [9] in which the angular correlation of two Compton-scattered **photons** arising from e^+e^- annihilation are measured
- The violation of Bell inequality was demonstrated in 1970s using entangled **photons** [10–12], confirming the non-locality of our universe
- Alain Aspect, John Clauser and Anton Zeilinger won the Nobel Prize in Physics in 2022 for demonstrating the potential to investigate and control particles (**photons**) that are in entangled states [13]

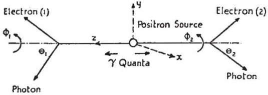

FIG. Angular correlation effects [14] demonstrated by the Wu-Shaknov Experiment

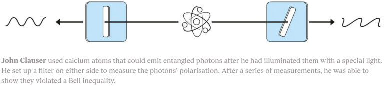

FIG. Clauser's photon entanglement experiment [13]

Relevant activities

- 20'+10' oral report in *Quantum Observables for Collider Physics 2025*
- 20' oral report in *Workshop on Quantum Entanglement at the Energy Frontier* (scheduled on Apr 26)
- 30' oral report in *Muon4Future 2025* (scheduled on May 26–30)

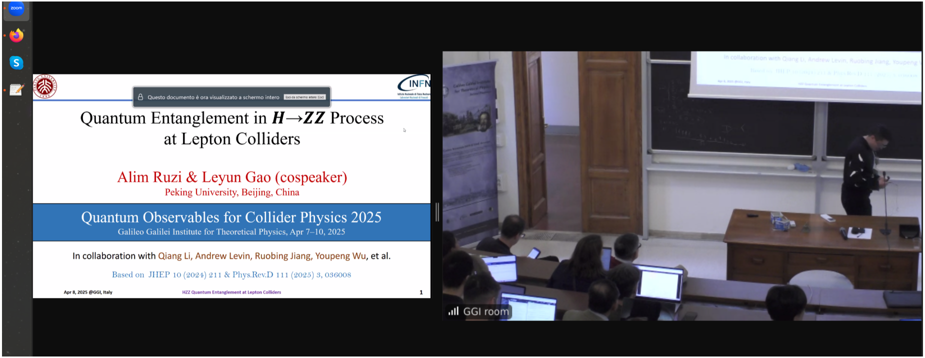

PKMuon quantum entanglement experiment prospects

- GeV-scale muon and positron on-target experiments are examined as **controllable entangled lepton pair sources** through the kinematic approach
- Quantum entanglement and the CHSH inequality violation are present in the primary scattering products
- A **first measurement of the correlation between entangled free-traveling lepton pairs** is proposed to verify the entanglement
- The electron-positron beam polarization correlation measurement can be conducted with **a high event rate at many domestic positron beam facilities**

Process	Incident flux	Primary event rate	Secondary coincidence rate
$\mu^- e^- \to \mu^- e^-$	$10^5/\mathrm{s}$	$2.6 \times 10^4/\mathrm{d}$	(not estimated)
$e^+ e^- \to e^+ e^-$	$10^5/\mathrm{s}$	$1.9 \times 10^2/\mathrm{s}$	$4.4 \times 10^2/\mathrm{y}$
$e^+ e^- \to e^+ e^-$	$10^{12}/\mathrm{s}$*	$\mathbf{1.9 \times 10^9/s}$	$\mathbf{1.4 \times 10^2/s}$

*Possibly from the beam dump of the STCF.